A New Class of Biomimetically Relevant "Scorpionate" Ligands. 1. The (2-Hydroxyphenyl)bis(pyrazolyl)methanes: Synthesis and Structural Characterization of Some Cobalt(II) Complexes

Timothy C. Higgs and Carl J. Carrano*

Department of Chemistry, Southwest Texas State University, San Marcos, Texas 78666

Received August 30, 1996[⊗]

The syntheses of a new class of potentially biomimetic, tripodal, mixed functionality ligands, (2-hydroxyphenyl)bis(pyrazolyl)methane (L1), (2-hydroxyphenyl)bis(3,5-dimethylpyrazolyl)methane (L2), and (2-hydroxyphenyl)bis(3-isopropylpyrazolyl)methane (L3), are described. These ligands have been used to prepare the cobalt(II) complexes $[Co(L1)_2]\cdot 2.5MeOH\cdot 1.5H_2O$, **1**·2.5MeOH·1.5$H_2O$; $[Co(L2)_2]\cdot 0.5H_2O$, **2**·0.5H_2O; $[Co(L3)Cl_2]$, **3**; and $[Co_3(\mu_3\text{-}OH)_2(\mu\text{-}L3)_2(L3)(H_2O)]BF_4$, **4**. X-ray structural analysis of **1**−**4** gave the following structural parameters: **1**, $C_{30}H_{34}N_8CoO_6$, triclinic, $a = 8.286(2)$ Å, $b = 10.053(3)$ Å, $c = 10.562(2)$ Å, $\alpha = 109.66(2)°$, $\beta = 96.57(1)°$, $\gamma = 91.11(3)°$, space group $P\bar{1}$, $Z = 1$; **2**, $C_{38}H_{38}N_8CoO_6$, triclinic, $a = 8.746(5)$ Å, $b = 10.900(5)$ Å, $c = 11.399(8)$ Å, $\alpha = 70.82(4)°$, $\beta = 75.13(5)°$, $\gamma = 81.46(4)°$, space group $P\bar{1}$, $Z = 1$; **3**, $C_{20}H_{26}N_4Cl_4CoO$, monoclinic, $a = 10.934(2)$ Å, $b = 12.404(2)$ Å, $c = 19.267(3)$ Å, $\beta = 98.33(1)°$, space group $P2_1/n$, $Z = 4$; **4**, $C_{58}H_{70}N_{12}BCo_3F_4O_9$, monoclinic, $a = 14.798(5)$ Å, $b = 23.657(8)$ Å, $c = 20.614(7)$ Å, $\beta = 97.75(2)°$, space group $P2_1/n$, $Z = 4$.

Introduction

Since the initial development of tris(pyrazolyl)borate or "scorpionate" ligands by Trofimenko and others in the late 1960s,[1,2] they have found wide application in coordination, organometallic, and bioinorganic chemistry. They have been particularly valuable in the biomimetic coordination chemistry of numerous metalloproteins since these monoanionic, facially coordinating ligands have histidine-like donors which can hold three *cis* sites fixed while leaving other coordination sites open. Important examples include the work of Kitajima *et al*. with the hindered ligand hydrotris(3,5-diisopropylpyrazolyl)borate and copper(II), with which these workers have produced excellent structural and spectroscopic models of the oxygenated form of the oxygen transport protein, hemocyanin,[3,4] and of the active site of "blue" or type I cupredoxins.[5,6] Other successes include the work of Lippard *et al.* with the unsubstituted ligand, hydrotris(pyrazolyl)borate, to produce μ-oxo−bis(μ-carboxylato)−Fe(III) or −Mn(III) dimeric systems, which have strong structural similarities to the active sites of various oxo-bridged dinuclear centers in metalloproteins such as hemerthyrin, ribonucleotide reductase, methane monooxygenase, and pseudocatalase.[7]

Despite their advantages, the tris(pyrazolyl)borate ligands are completely symmetric with all nitrogen donors and many metalloprotein active sites do not have such monofunctional ligand atom donor spheres. Thus, it would be expedient to be able to synthesize polyfunctional tridentate ligands containing two pyrazole groups which also incorporate other biologically relevant ligands (thiols, phenols, carboxylates, etc.). Using a synthesis based on that of Peterson *et al.*[8−10] for the formation of dipyrazolylalkanes starting from bis(pyrazolyl) ketones and aliphatic or aromatic carbonyl compounds, we have developed a strategy for producing a new class of mixed-functionality ligands which retain all the considerable advantages of tris(pyrazolyl)borate ligands, *i*.e., easily synthesized, tridentate, facially coordinating, and monoanionic. This scheme has been used by Canty *et al.*[11] to synthesize a series of all nitrogen functionality, imidazole/pyrazole, imidazole/pyridine, and pyrazole/pyridine ligands, but as yet there have been no reports of its use to produce mixed-functionality species such as those described here. The new ligands described here are related to tris(pyrazolyl)methane, but with one of the pyrazole groups replaced by a phenol, thiophenol, benzenecarboxylic acid, or other functionalized phenyl group. Steric hindrance is easily incorporated into the ligands *via* the pyrazole rings, giving considerable control with respect to their potential coordinative ability with transition metal ions.

This paper describes the full synthesis and characterization of the L1, L2, and L3 ligands (Scheme 1). In addition, as part of our initial investigations into the transition metal coordination chemistry of this new class of ligands, their reactivity with the divalent transition metal ion, Co(II), has been probed.

Experimental Section

All operations were carried out in air unless otherwise stated. THF was freshly distilled from sodium/benzophenone while diethyl ether was anhydrous 99.8% (Aldrich Chemical Co.) and used as received.

[⊗] Abstract published in *Advance ACS Abstracts,* January 1, 1997.

(1) Trofimenko, S. *J. Am. Chem. Soc.* **1967**, *89*, 3170.
(2) Trofimenko, S. *J. Am. Chem. Soc.* **1967**, *89*, 6288.
(3) Kitajima, N.; Fujisawa, K.; Moro-oka, Y. *J. Am. Chem. Soc.* **1989**, *111*, 8975.
(4) Kitajima, N.; Fujisawa, K.; Fujimoto, C.; Moro-oka, Y.; Hashimoto, S.; Kitagawa, T.; Toriumi, K.; Tatsumi, K.; Nakamura, A. *J. Am. Chem. Soc.* **1992**, *114*, 1277.
(5) Kitajima, N. *Adv. Inorg. Chem.* **1992**, *39*, 1.
(6) Kitajima, N.; Fujisawa, K.; Tanaka, M.; Moro-oka, Y. *J. Am. Chem. Soc.* **1992**, *114*, 9232.
(7) (a) Armstrong, W. H.; Spool, A.; Papaefthymiou, G. C.; Frankel, R. B.; Lippard, S. J. *J. Am. Chem. Soc.* **1984**, *106*, 3653 and references therein. (b) Sheats, J. E.; Czernuszewicz, R. S.; Dismukes, G. C.; Rheingold, A. L.; Petrouleas, V.; Stubbe, J.; Armstrong, W. H.; Beer, R. H.; Lippard, S. J. *J. Am. Chem. Soc.* **1987**, *109*, 1435.
(8) The, K. I.; Peterson, L. K. *Can. J. Chem.* **1973**, *51*, 422.
(9) The, K. I.; Peterson, L. K.; Kiehlmann, E. *Can. J. Chem.* **1973**, *51*, 2448.
(10) Peterson, L. K.; Kiehlmann, E.; Sanger, A. R.; The, K. I. *Can. J. Chem.* **1974**, *52*, 2367.
(11) Byers, P. K.; Canty, A. J.; Honeyman, R. T. *J. Organomet. Chem.* **1990**, *385*, 417.

S0020-1669(96)01070-1 CCC: $14.00

Scheme 1[a]

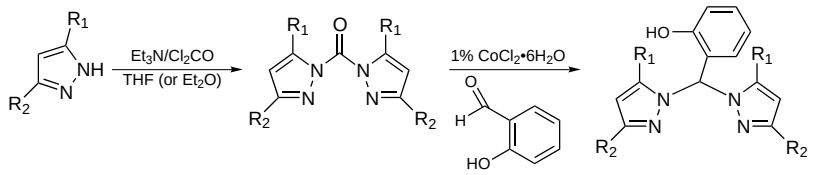

[a] L1; R_1 = H; R_2 = H. L2: R_1 = Me; R_2 = Me. L3: R_1 = H; R_2 = ^{i}Pr.

Other solvents used were of reagent grade (Aldrich). Microanalyses were performed by Desert Analytics Laboratory, Tucson, AZ. ^{1}H and ^{13}C NMR spectra were obtained using an IBM Instruments 80 MHz FT-NMR. IR spectra were recorded in KBr disks on a Perkin-Elmer 1600 series FTIR. Solution electronic spectra were performed on a Hewlett-Packard 8452A diode array spectrophotometer under the computer control of a Compaq Deskpro 386S with OLIS model 4300 data system diode array spectrophotometry software (On-line Instruments Inc.). Cyclic voltammetry data was acquired using a Bioanalytical Systems Inc., CV-27 cyclic voltammograph, with platinum working and secondary electrodes, a Ag/0.01 M $AgNO_3$ (in MeCN) BAS nonaqueous reference electrode, and [^{n}Bu$_4$N][PF$_6$] as an electrolyte. Room temperature magnetic moments were measured on a Johnson Matthey JME magnetic susceptibility balance using Pascal's constants for diamagnetic corrections.

Ligand Synthesis. (2-Hydroxyphenyl)bis(pyrazolyl)methane, L1. (a) Bis(pyrazolyl) Ketone. This was prepared according to the procedure described by Canty *et al.*[11] Yield: 85%.

(b) (2-Hydroxyphenyl)bis(pyrazolyl)methane. Bis(pyrazolyl) ketone (4.40g, 28.2 mmol) was placed in a 100 cm^3 round-bottomed flask which was purged and filled with nitrogen (twice). Salicylaldehyde (3.45 g, 28.2 mmol) and $CoCl_2$·6H_2O (0.03 g, 0.13 mmol) were added to the flask. The mixture was then heated to 80 °C and vigorously stirred until it set, during which time the mixture turned dark blue and evolution of CO_2 was observed. The mixture was allowed to cool to room temperature before CH_2Cl_2 (30 cm^3) was added and the flask shaken until a pink solution had formed. This solution was extracted with H_2O (2 × 30cm^3), which removed the pink coloration from the organic layer, which was separated and dried over $MgSO_4$ for 16 h. Hexane (50 cm^3) was then added to the solution, and the CH_2Cl_2 component was removed by rotary evaporation, causing the precipitation of a pale beige solid. The flask containing the solid suspended in hexane was placed in an ultrasound bath for 30 min to break up the lumps which had formed, yielding a white microcrystalline solid. This solid was collected by filtration, washed with hexane (20 cm^3) and dried *in vacuo*. Yield: 3.70 g, 55%. Anal. Calcd for $C_{13}H_{12}N_4O$: C, 65.0; H, 5.0; N, 23.3. Found: C, 64.3; H, 4.86; N, 23.09. ^{1}H NMR (80 MHz, d_6-acetone): δ 6.31 (t, 2H, 4-pzH), 6.78−7.45 (m, 4H, PhH), 7.57 (d, 4H, 3,5-pzH), 7.77 (s, 1H, CH). IR (cm^{-1}): 3126, 3105, 1607, 1507, 1461, 1401, 1350, 1307, 1267, 1234, 1179, 1159, 1087, 1056, 979, 966, 916, 873, 813, 799, 760, 627, 609.

(2-Hydroxyphenyl)bis(3,5-dimethylpyrazolyl)methane, L2. (a) Bis(3,5-dimethylpyrazolyl) Ketone. The procedure of Canty *et al.*[11] was used for preparing bis(pyrazolyl) ketone, except 3,5-dimethylpyrazole (7.066 g, 73.5 mmol) was substituted for pyrazole, and anhydrous THF (200 cm^3) was used as the solvent instead of anhydrous diethyl ether. The final product was a white microcrystalline solid. Yield: 5.85 g, 73%.

(b) (2-Hydroxyphenyl)bis(3,5-dimethylpyrazolyl)methane. The same procedure was used as for (2-hydroxyphenyl)bis(pyrazolyl)-methane (*vide supra*), using the following reagents and reactant ratios: bis(3,5-dimethylpyrazolyl) ketone (4.00 g, 18.3 mmol), salicylaldehyde (2.23 g, 18.3 mmol), $CoCl_2$·6H_2O (0.03 g, 0.13 mmol). Yield: 2.49 g, 46%. Anal. Calcd for $C_{17}H_{20}N_4O$: C, 68.9; H, 6.8; N, 18.9. Found: C, 68.55; H, 6.86; N, 18.84. ^{1}H NMR (80 MHz, d_4-MeOH): δ 2.06 (s, 6H, CH_3), 2.15 (s, 6H, CH_3), 5.91 (s, 2H, 4-pzH), 6.6−7.0 (m, 3H, PhH), 7.1−7.3 (m, 1H, PhH), 7.66 (s, 1H, CH). IR (cm^{-1}): 2923, 2707, 2598, 1608, 1552, 1508, 1463, 1417, 1376, 1321, 1294, 1266, 1209, 1155, 1098, 974, 885, 795, 756, 688, 624, 546.

(2-Hydroxyphenyl)bis(3-isopropylpyrazolyl)methane, L3. (a) Bis(3-isopropylpyrazolyl) Ketone. This was prepared using the method of Canty *et al.*[11] but using 3-isopropylpyrazole (8.085 g, 73.5 mmol) and anhydrous THF (200 cm^3) as the solvent, although the final workup also had to be modified since the bis(3-isopropylpyrazolyl) ketone is an oil. Yield: 7.5 g, 83%. The product was used immediately in the next stage of the synthesis without further purification.

(b) (2-Hydroxyphenyl)bis(3-isopropylpyrazolyl)methane. Bis(3-isopropylpyrazolyl) ketone (7.0 g, 28.5 mmol) was placed in a 100 cm^3 flask which was purged with nitrogen (twice). Salicylaldehyde (10.44 g, 85.5 mmol) and $CoCl_2$·6H_2O (0.05 g, 0.21 mmol) were added to the flask. The mixture was stirred vigorously and heated to 120 °C for 45−60 min during which time the mixture turned dark blue and slow evolution of CO_2 was observed. Once the evolution CO_2 had ceased, the reaction mixture was allowed to cool to room temperature. The resultant thick blue oil was dissolved in CH_2Cl_2 (25 cm^3), forming a red/pink solution. This was extracted with H_2O (4 × 100 cm^3 portions), removing the red/pink color from the organic layer. The CH_2Cl_2 layer was then separated and then evaporated to dryness under a reduced pressure to yield a brown oil. The excess salicylaldehyde in the oil was distilled off under a reduced pressure and the resultant thick dark brown oil was then dissolved in hexane (20 cm^{-3}). The hexane solution was stirred for several hours, during which time a large quantity of a white microcrystalline solid was deposited, forming a thick suspension. Once the precipitation appeared to cease, the solid was collected by filtration, washed with hexane (2 × 10 cm^3), and dried *in vacuo*. Yield: 3.2 g, 35%. Anal. Calcd for $C_{19}H_{24}N_4O$: C, 70.4; H, 7.4; N, 17.3. Found: C, 70.18; H, 7.47; N, 17.31. ^{1}H NMR (80 MHz, *d*-$CHCl_3$): δ 1.2 (d, 12H, CH_3), 2.94 (p, 2H, CH), 6.05 (d, 2H, 4-pzH), 6.7−7.3 (m + s, 5H, PhH(m) + CH(s)), 6.65 (d, 2H, 5-pzH), 12.29 (s, 1H, Ph-OH). IR (cm^{-1}): 3052, 2960, 2870, 2728, 2606, 1605, 1519, 1458, 1382, 1322, 1291, 1266, 1205, 1099, 1069, 1043, 876, 816, 790, 755, 720, 634.

The ^{13}C NMR spectra of L1, L2, and L3 in $CDCl_3$ are summarized in Table 1.

Table 1. ^{13}C-NMR Characterization of the (2-Hydroxyphenyl)bis(pyrazolyl)methane Ligands L1, L2, and L3 in $CDCl_3$

peak positions (ppm)			
L1	L2	L3	proposed assignment
	11.115		5-pyrazole-Me
	13.530		3-pyrazole-Me
		22.526	3-pyrazole-*i*-Pr C−H
		27.707	3-pyrazole-*i*-Pr CH_3
76.998	73.279	77.007	bridgehead C−H
106.191	106.968	102.880	pyrazole C4
118.626	118.594	118.909	phenolate C−H
119.872	119.548	119.580	phenolate C−H
121.287	*a*	121.661	phenolate C1′ (bridgehead)
129.699	129.799	130.208	phenolate C−H
130.203	140.400	130.511	pyrazole C5
131.574	130.733	131.317	phenolate C−H
140.530	148.244	160.183	pyrazole C3
155.098	155.514	155.440	phenolate C−O (C2′)

[a] Not observed, possibly buried under phenolate C−H, 119.548, 118.595 peaks.

Cobalt(II) Complexes. 1·2.5MeOH·1.5H$_2$O. L1 (0.20 g, 0.833 mmol) was dissolved in MeOH (15 cm^3), forming a colorless solution. NaOMe (0.045 g, 0.833 mmol) was added to the solution which was stirred until it dissolved. $CoCl_2$·6H_2O (0.0991 g, 0.417 mmol) was then added to the solution, which instantly changed to a dark blue color before dissolving, forming a red/purple solution. The mixture was stirred for 30 min at room temperature, before being allowed to stand. Over a period of days very large orange crystals formed in the solution, as well as a small amount of a microcrystalline dark blue material. The large orange crystals were picked out individually using a Pasteur

Table 2. Crystallographic Data and Data Collection Parameters for L1, **1**−**4**

parameter	L1·MeCN	**1**·4MeOH	**2**·4MeOH	**3**·CH_2Cl_2	**4**·MeOH·4H_2O
formula	$C_{15}H_{12}N_5O$	$C_{30}H_{34}N_8CoO_6$	$C_{38}H_{38}N_8CoO_6$	$C_{20}H_{26}N_4Cl_4CoO$	$C_{58}H_{70}N_{12}B_1F_4Co_3O_9$
space group	$P2_1$	$P\bar{1}$	$P\bar{1}$	$P2_1/c$	$P2_1/c$
a, Å	8.931(1)	8.286(2)	8.746(5)	10.934(2)	14.798(5)
b, Å	8.718(1)	10.053(3)	10.900(5)	12.404(2)	23.657(8)
c, Å	9.539(1)	10.562(2)	11.399(8)	19.267(3)	20.614(7)
α, deg		109.66(2)	70.82(4)		
β, deg	92.29(2)	96.57(1)	75.13(5)	98.33(1)	97.75(2)
γ, deg		91.11(3)	81.46(4)		
V, Å^3	742.13(10)	821.57(50)	989.6(12)	2585.64(78)	7150.7(60)
ρ, g cm^{-3}	1.245	1.337	1.278	1.385	1.247
Z	2	1	1	4	4
fw	278.3	330.8	761.7	539.2	1342.9
cryst size, mm	0.4 × 0.2 × 0.2	0.5 × 0.5 × 0.3	0.4 × 0.2 × 0.1	0.7 × 0.4 × 0.2	0.4 × 0.4 × 0.3
cryst color, habit	colorless, block	orange, block	yellow, rod	blue, block	red/orange, block
μ, mm^{-1}	0.084	0.576	0.487	1.095	0.754
no. of unique data	1204	2111	2483	3350	6574
no. of obs data $F > 4.0\sigma(F)$	952	1878	1475	2100	3886
data:param ratio	5.0:1	9.2:1	6.1:1	7.7:1	4.8:1
transm factors	0.8376/0.8647	0.827/0.965	0.7289/0.9046	na[c]	na
R[b]	4.82	3.75	7.03	5.12	7.35
R_w[b]	5.67	5.33	8.47	5.91	10.52
max difference peak, e Å^{-3}	+0.26	+0.36	+0.43	+0.42	+0.62
Δ/*σ*(mean)	0.007	0.001	0.001	0.001	0.007

[a] Temp, 298 K; radiation, Mo Kα; scan type, $\theta-2\theta$; data collection range, 3.5−45.0°. [b] Quantity minimized $\omega w(F_o - F_c)^2$; $R = \sum|F_o - F_c|/\omega F_o$; $R_w = (\omega w(F_o - F_c)^2/\sum(\omega F_o)^2)^{1/2}$.

pipet, one of which was used for the X-ray crystal structure determination (*vide infra*), and the others were dried *in vacuo*. Yield: 0.12 g, 27%. Anal. Calcd for $C_{26}H_{22}N_8CoO_2$·2.5MeOH·1.5H_2O: C, 53.11; H, 5.43; N, 17.39. Found: C, 53.01; H, 5.35; N, 17.37. IR (cm^{-1}): 3386, 3118, 1594, 1553, 1509, 1482, 1444, 1404, 1327, 1288, 1200, 1156, 1095, 1062, 1024, 984, 901, 806, 756, 724, 630, 614, 577, 523.

2·0.5H_2O. L2 (0.20 g, 0.68 mmol) was dissolved in MeOH (15 cm^3), and to this solution was added NaOMe (0.0365 g, 0.68 mmol). $CoCl_2$·6H_2O (0.0804 g, 0.337 mmol) was added to the reaction mixture, initially turning dark blue before dissolving to form a red/orange solution. The mixture was refluxed for 10 min, during which time a pale yellow microcrystalline solid precipitated from the solution. The reaction mixture was allowed to cool to room temperature, and the yellow solid was collected by filtration, washed with MeOH (2 cm^3) and diethyl ether (5 cm^3), and dried *in vacuo*. Yield: 0.12 g, 54%. The red/orange filtrate was left to stand for several days, yielding another crop of pale yellow block crystals, which were used in the X-ray structure determination (*vide infra*). Anal. Calcd for $C_{34}H_{38}N_8CoO_2$·0.5H_2O: C, 62.01; H, 5.93; N, 17.02. Found: C, 61.98; H, 5.90; N, 16.82. IR (cm^{-1}): 3422, 3052, 2913, 1594, 1559, 1483, 1418, 1385, 1351, 1321, 1275, 1246, 1162, 1147, 1112, 1038, 984, 903, 860, 799, 749, 734, 696, 595, 582, 525, 492, 468.

3. L3 (0.30 g, 0.926 mmol) was dissolved in MeCN (20 cm^3), forming a colorless solution. To this was added anhydrous $CoCl_2$, which rapidly dissolved, forming a deep blue solution. The reaction mixture was stirred at room temperature for 10 min, before being left to stand. Over a period of days large block-like, dark blue crystals formed in the solution, which were collected by filtration, washed with diethyl ether (5 cm^3), and dried *in vacuo*. Yield: 0.13 g, 64%. Anal. Calcd for $C_{19}H_{24}N_4Cl_2CoO$: C, 50.2; H, 5.3; N, 12.3. Found: C, 49.64; H, 5.29; N, 12.16. IR (cm^{-1}): 3414, 3107, 2964, 2872, 2719, 2586, 1598, 1521, 1480, 1460, 1445, 1388, 1363, 1342, 1266, 1240, 1199, 1159, 1077, 1051, 1021, 903, 606, 755, 724, 653.

4. L3 (0.30 g, 0.926 mmol) was dissolved in MeOH (15 cm^3). NaOMe (0.050 g, 0926 mmol) was added to the solution, which upon dissolution caused a color change from colorless to deep yellow. $Co(BF_4)_2$·6H_2O (0.2996 g, 0.88 mmol) was then added, producing a red/orange solution. The reaction mixture was refluxed for 20 min, then cooled to room temperature and allowed to stand. Over a period of days large red/orange block-like crystals formed in the solution. One of these was used for the crystallographic investigation (*vide infra*) while the remainder were collected by filtration, washed with diethyl ether (10 cm^3), and dried *in vacuo*. Yield: 0.95g, 24%. Anal. Calcd for $C_{57}H_{74}N_{12}BCo_3F_4O_6$: C, 53.2; H, 5.8; N, 13.1. Found: C, 53.19; H, 5.56; N, 12.93. IR (cm^{-1}): 3448, 3144, 2966, 2928, 2870, 1596, 1560, 1526, 1482, 1444, 1390, 1363, 1345, 1316, 1286, 1240, 1202, 1156, 1120, 1084, 1052, 1020, 903, 859, 834, 808, 769, 726, 653, 589, 550.

Table 3. Bond Distances (Å) and Angles (deg) for **1**·4MeOH

Distances			
Co1−N1	2.133(2)	Co1−N3	2.117(3)
Co1−O1	2.016(2)	Co1−N1A	2.133(2)
Co1−N3A	2.117(3)	Co1−O1A	2.016(2)
Angles			
N1−Co1−N3	93.3(1)	N1−Co1−O1	90.8(1)
N3−Co1−O1	89.9(1)	N1−Co1−N1A	180.0(1)
N3−Co1−N1A	86.8(1)	O1−Co1−N1A	89.2(1)
N1−Co1−N3A	86.8(1)	N3−Co1−N3A	180.0(1)
O1−Co1−N3A	90.1(1)	N1A−Co1−N3A	93.3(1)
N1−Co1−O1A	89.2(1)	N3−Co1−O1A	90.1(1)
O1−Co1−O1A	180.0(1)	N1A−Co1−O1A	90.8(1)
N3A−Co1−O1A	89.9(1)		

Crystallography. Crystals of L1 suitable for crystallographic investigation were grown from a saturated MeCN solution while those of **1**, **2**, and **4** were obtained from the reaction mixture mother liquor as described in the Experimental Section (*vide supra*). Crystals of **3** were obtained by layering a CH_2Cl_2 solution of **3** with isopropyl ether as a countersolvent. All crystals were sealed in thin-walled quartz capillaries to prevent loss of lattice solvent. The crystals were mounted on a Siemens P4 diffractometer with a sealed-tube Mo X-ray source (λ = 0.710 73 Å) and computer controlled with installed Siemens XSCANS 2.1 software. Automatic searching, centering, indexing, and least-squares routines were carried out for L1 and **1**−**4** with at least 25 reflections in the range $25° \le 2\theta \le 20°$ used to determine unit cell parameters. During data collection, the intensities of three representative reflections were monitored every 97 reflections, but in no case was any serious decay observed. The data were corrected for Lorentz and polarization effects and for crystals L1, **1**, and **2** for absorption, using a semiempirical correction determined from *ψ*-scan data. Structure solutions for L1 and **1**−**4** were obtained either by direct methods or *via* the Patterson function, and refinement by difference Fourier synthesis was accomplished using the Siemens SHELXTL-PC[12] software package. A summary of cell parameters, data collection conditions, solution type, and refinement results can be found in Table 2 with selected bond lengths and angles given in Tables 3−6. Details pertinent to the individual refinements are outlined below.

L1·MeCN was solved by direct methods revealing one molecule of L1 and one MeCN lattice solvent molecule per asymmetric unit. All

(12) Sheldrick, G. M. *SHELXTL-PC*, Version 4.1; Siemens X-ray Analytical Instruments, Inc.: Madison, WI, 1989.

Table 4. Bond Distances (Å) and Angles (deg) for **2**·4MeOH

	Distances		
Co1−N1	2.118(7)	Co1−N3	2.136(10)
Co1−O1	2.023(6)	Co1−N1A	2.118(7)
Co1−N3A	2.136(10)	Co1−O1A	2.023(6)
	Angles		
N1−Co1−N3	97.3(3)	N1−Co1−O1	88.4(3)
N3−Co1−O1	92.9(3)	N1−Co1−N1A	180.0(1)
N3−Co1−N1A	82.7(3)	O1−Co1−N1A	91.6(3)
N1−Co1−N3A	82.7(3)	N3−Co1−N3A	180.0(1)
O1−Co1−N3A	87.1(3)	N1A−Co1−N3A	97.3(3)
N1−Co1−O1A	91.6(3)	N3−Co1−O1A	87.1(3)
O1−Co1−O1A	180.0(1)	N1A−Co1−O1A	88.4(3)
N3A−Co1−O1A	92.9(3)		

Table 5. Bond Distances (Å) and Angles (deg) for **3**·CH_2Cl_2

	Distances		
Co1−Cl1	2.216(2)	Co1−Cl2	2.243(2)
Co1−N1	2.033(5)	Co1−N3	2.021(5)
	Angles		
Cl1−Co1−Cl2	109.9(1)	Cl1−Co1−N1	115.1(2)
Cl2−Co1−N1	110.1(2)	Cl1−Co1−N3	117.3(2)
Cl2−Co1−N3	109.7(2)	N1−Co1−N3	93.8(2)

non-hydrogen atoms including the MeCN solvent molecule were refined anisotropically. The hydrogen atoms were included in calculated positions (except for the MeCN molecule where no hydrogen atoms were either calculated or located by refinement) using a riding model and fixed isotropic thermal parameters.

1·4MeOH and **2**·4MeOH were solved by the Patterson method, which indicated that the asymmetric unit contains one half-molecule of **1** or **2**, respectively, with the Co atom sitting on an inversion center. Initial isotropic, followed by anisotropic, refinement of the non-hydrogen atoms revealed the presence of two molecules of MeOH per half-molecule of **1** and **2**, and these were also refined ansiotropically. The hydrogen atoms were included in calculated positions using a riding model and fixed isotropic thermal parameters.

The structure of **3**·CH_2Cl_2 was solved by direct methods; the asymmetric unit containing one molecule of **3**. Subsequent isotropic refinement and difference maps located one CH_2Cl_2 molecule per **3**. All non-hydrogen atoms were refined anisotropically with hydrogen atoms included in calculated positions using a riding model and fixed isotropic thermal parameters.

4·MeOH·$4H_2O$ was again solved by direct methods. The initial E-map revealed one $[Co_3(\mu_3\text{-}OH)_2(\mu\text{-}L3)_2(L3)(H_2O)]^+$ (**4c**) cation and one $[BF_4]^-$ anion. Isotropic, followed by anisotropic, refinement of the non-hydrogen atoms of **4c** and $[BF_4]^-$ groups coupled with difference maps revealed the presence of an additional molecule of lattice MeOH and four lattice H_2O molecules. All the non-hydrogen atoms were anisotropically refined to convergence, with hydrogen atoms included in calculated positions (except for the lattice solvent molecules) using a riding model and fixed isotropic thermal parameters.

Results

Description of Structures. L1·MeCN. This compound contains discrete units of the (2-hydroxyphenyl)bis(pyrazolyl)-methane L1, ligand and one molecule of lattice MeCN. The pyrazole rings of the L1 ligand are orientated in a quasi-antiparallel manner with respect to each other, presumably to minimize intramolecular steric interaction between the N1 and N2 atoms of the two rings (Figure 1). Symmetry expansion of the asymmetric unit reveals that each L1 molecule is intermolecularly hydrogen bonded to two adjacent L1 molecules in the crystal lattice *via* the phenol O−H (O1) group of one L1 molecule and the N4a pyrazole of the other, forming infinite hydrogen bonded chains (O1···N4a separation: 2.688 Å). The orientation of the phenol group within each L1 molecule, approximately perpendicular to the two pyrazole rings, may be mediated by this extended hydrogen-bonded network.

1·4MeOH and 2·4MeOH. The asymmetric units of these two structures both contain one half-molecule of the neutral

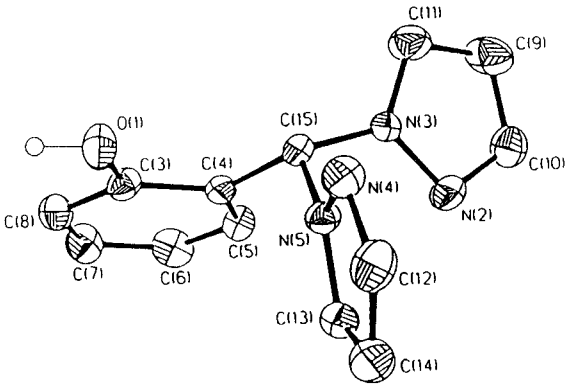

Figure 1. (a) ORTEP view of two adjacent L1 molecules, with 30% probability thermal ellipsoids and full atomic labeling.

Table 6. Bond Distances (Å) and Angles (deg) for **4**·MeOH·$4H_2O$

	Co1 Distances		
Co1−O4	1.998(9)	Co1−O3	2.016(8)
Co1−O6	2.132(7)	Co1−O5	2.156(7)
Co1−N11	2.152(10)	Co1−N9	2.125(12)
	L−Co1−L Angles		
O3−Co1−O4	175.7(4)	O4−Co1−O5	93.2(3)
O3−Co1−O5	83.2(3)	O3−Co1−O6	82.8(3)
O4−Co1−O6	93.8(4)	O5−Co1−O6	69.8(2)
O4−Co1−N9	93.7(4)	O3−Co1−N9	89.3(4)
O6−Co1−N9	169.2(3)	O5−Co1−N9	102.0(4)
O3−Co1−N11	91.2(4)	O4−Co1−N11	91.8(4)
O5−Co1−N11	167.9(3)	O6−Co1−N11	98.9(3)
N9−Co1−N11	88.9(4)		
	Co2 Distances		
Co2−O2	2.002(8)	Co2−O3	2.005(9)
Co2−O5	2.160(7)	Co2−O6	2.166(6)
Co2−N6	2.093(11)	Co2−N8	2.123(10)
	L−Co2−L Angles		
O2−Co2−O3	162.0(3)	O2−Co2−O5	83.1(3)
O3−Co2−O5	83.4(3)	O2−Co2−O6	82.0(3)
O3−Co2−O6	82.2(3)	O5−Co2−O6	69.1(2)
O2−Co2−N6	91.7(4)	O3−Co2−N6	102.2(4)
O5−Co2−N6	99.2(3)	O6−Co2−N6	167.2(3)
O2−Co2−N8	92.3(4)	O3−Co2−N8	98.8(4)
O5−Co2−N8	168.9(3)	O6−Co2−N8	100.3(3)
N6−Co2−N8	91.0(4)		
	Co3 Distances		
Co3−O1	1.997(7)	Co3−O2	2.069(7)
Co3−O5	2.166(6)	Co3−O6	2.192(6)
Co3−N2	2.134(10)	Co3−N4	2.140(11)
	L−Co3−L Angles		
O2−Co3−O5	81.4(3)	O1−Co3−O2	173.5(3)
O1−Co3−O6	94.3(3)	O1−Co3−O5	93.9(3)
O5−Co3−O6	68.5(2)	O2−Co3−O6	79.8(3)
O1−Co3−N2	89.3(3)	O2−Co3−N2	95.9(3)
O5−Co3−N2	100.8(4)	O6−Co3−N2	168.9(4)
O2−Co3−N4	96.3(4)	O1−Co3−N4	87.5(4)
O6−Co3−N4	100.7(3)	O5−Co3−N4	169.2(3)
N2−Co3−N4	90.0(4)		
	Co···Co Distances		
Co1···Co2	2.848	Co2···Co3	2.915
Co1···Co3	3.384		
	Co−L−Co Angles		
Co1−O3−Co2	90.2(3)	Co2−O2−Co3	91.5(3)
Co1−O5−Co3	103.0(2)	Co1−O5−Co2	82.6(2)
Co1−O6−Co2	83.0(2)	Co2−O5−Co3	84.7(2)
Co1−O6−Co3	84.0(2)	Co1−O6−Co3	103.0(3)

complex $[Co(L1)_2]$, **1**, or $[Co(L2)_2]$, **2**, and two molecules of lattice MeOH. Each molecule of **1** and **2** consists of one Co(II) atom with two ligands coordinated in a tripodal, tridentate fashion, the coordination number of the metal atom in each complex molecule being 6 (Figures 2 and 3). The stereochem-

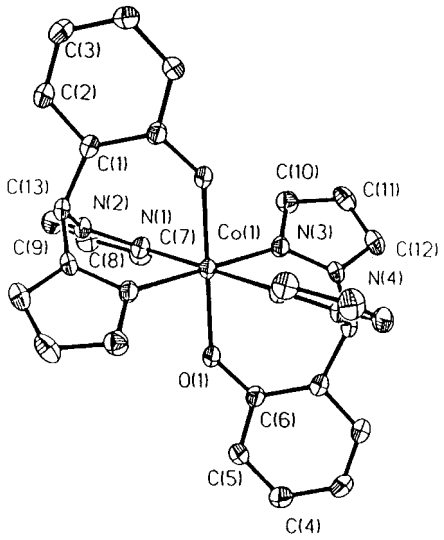

Figure 2. ORTEP view of a **1** molecule, with 20% probability thermal ellipsoids, showing selected atomic labeling.

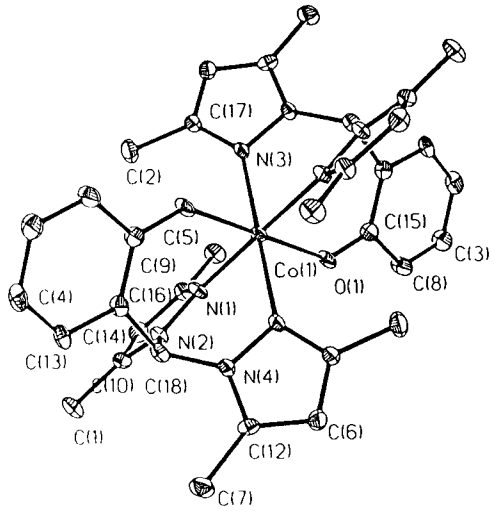

Figure 3. ORTEP view of a **2** molecule, with 20% probability thermal ellipsoids, showing selected atomic labeling.

istries of the Co(II) atoms in **1** and **2** can be described as flattened octahedral with the *trans*-axial Co-O bonds being short (2.016 Å for **1**, 2.023 Å for **2**) and the pyrazole to Co(II), Co−N_{pz} bonds which define the equatorial plane, rather longer (average distances: 2.125 Å for **1**, 2.127 Å for **2**). The L−Co−L *trans* angles are all 180° as required by the inversion symmetry within **1** and **2**. The other (*cis*) L−Co−L angles lie in the range 86.8(1)−93.3(1)° for **1** and 82.7(3)−97.3(3)°, *i.e.*, greater distortions from ideal for the more sterically crowded **2**.

3·CH_2Cl_2. The asymmetric units of this crystal structure contain discrete mononuclear units of the neutral complex, **3**. Each asymmetric unit also contains one molecule of lattice CH_2Cl_2. The Co(II) atom of **3** is coordinated to two pyrazole rings of an L3 ligand and to two chloride atoms and thus has a coordination number of 4 (Figure 4). The phenol group of the L3 ligand in **3** is uncoordinated but instead is weakly hydrogen bonded to a chloride atom (Cl2A) of an adjacent **3** molecule with a Cl···O separation of 3.172 Å. Thus, within the crystal, there are infinite, weakly hydrogen bonded chains of **3** molecules. The Co(II) stereochemistry can best be described as distorted tetrahedral. While the dihedral angle between the $CoCl_2$ and CoN_2 planes of 89.2° is close to the expected tetrahedral value, the individual L−Co−L bond angles show considerable deviations from the "ideal". For example, while the Cl−Co−Cl bond angle is 109.9(1)°, the N−Co−N angle is

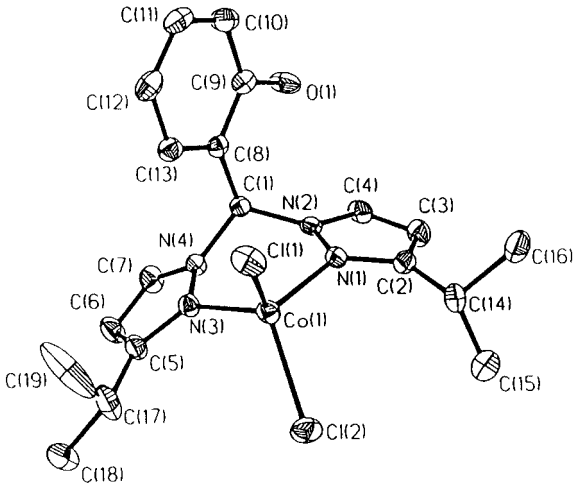

Figure 4. ORTEP view of a **3** molecule, with 20% probability thermal ellipsoids, showing full atomic labeling.

much smaller at 93.8(2)°, constrained by the "bite" of the bis-chelating L3 ligand. The Co−N_{pz} bonds (average distance: 2.027 Å) and Co−Cl bonds (average length: 2.223 Å) are within the range typically observed for these ligands in this coordination geometry. The shorter pyrazole−nitrogen bonds in **3** as compared to **1** and **2** are attributable to the tetrahedral stereochemistry of **3**·CH_2Cl_2 which allows a closer approach of the ligands to the Co(II) atom.

4·MeOH·4H_2O. This structure has an asymmetric unit containing a single discrete $[Co_3(\mu_3\text{-}OH)_2(\mu\text{-}L3)_2(L3)(H_2O)]$ cation, a BF_4 anion, one molecule of lattice MeOH, and four H_2O molecules. The cationic portion of **4**, **4c**, contains a constellation of 3 Co(II) atoms in a near isosceles triangular arrangement (Figure 5) with two short and one long Co···Co separation (short, 2.848 and 2.915 Å; long, 3.384 Å). The Co_3 core is bridged by two μ_3-OH groups, one displaced +1.225 Å (O5) above and the other −1.229 Å (O6) below the Co_3-plane. Each Co(II) atom of the **4** cation is coordinated to an L3 ligand, which binds in a facial, tridentate manner. The phenolate groups of the L3 ligands coordinated to Co1 and Co2 bridge to the cobalt atoms, Co2 and Co3, respectively, along the short sides of the approximate isosceles triangle of metal atoms. The phenolate (O1) of the L3 ligand of Co3 is terminally coordinated, but is intramolecularly hydrogen bonded to a water molecule (O4) bound to Co1 along the long side of the triangular Co_3 core (Figure 5), the O1···O4 separation being 2.455 Å (weak unsymmetrical hydrogen bonds typically have O···O separations in the range 2.7−3.0 Å[13]). Thus, the three Co(II) atoms in **4** have inequivalent, six-coordinate, highly distorted octahedral coordination environments (Figure 5). Each contains a $Co(\mu_3\text{-}OH)_2(pz\text{-}N)_2$ moiety, the four ligands of which are contained approximately within a single plane. In addition, Co2 is further bound to two *trans*-bridging phenolate groups (O2, O3), Co3 to one terminal (O1) and one bridging phenolate (O2), again *trans* orientated, and Co1 to one bridging phenolate (O3) and a H_2O (O4) solvent molecule. The Co−N_{pz} bond distances (Table 6) are similar to those observed in both **1** and **2**. The *trans* Co−O distances of the terminal and bridging phenolates and the coordinated water molecule are uniformly shorter than those of the Co−N_{pz} bonds and compare favorably with the *trans* Co−O bond lengths observed in **1** and **2** (*vide supra*). In contrast, the Co−(μ_3-OH) bonds, which are all *cis* orientated, are considerably longer (average distance: 2.162 Å, Table 6) than the *trans*-orientated Co−O bonds of **4c** and those of **1** and **2**. The L−Co−L bond angles, which define the coordination

(13) Novak, A. *Struct. Bonding (Berlin)* **1974**, *18*, 177.

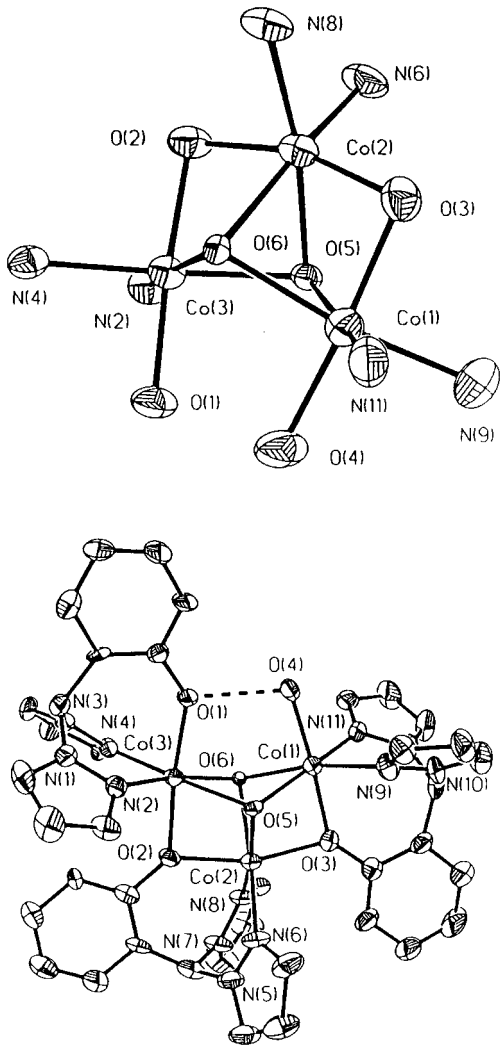

Figure 5. Lower: ORTEP view of the **4c** cation, with 20% probability thermal ellipsoids, showing selected atomic labeling and intramolecular hydrogen bonding. Upper: detailed view of the core structure of the **4c** cation.

geometries of the Co(II) atoms in **4c**, show significant distortions from those expected for an octahedral geometry (Table 6). For example, the *trans* L−Co−L angles of the ligands contained within the Co(μ_3-OH)$_2$(*pz*-N)$_2$ plane have an average value of 168.6°, a greater than 10° distortion from the "ideal" octahedral *trans* angle. This can be attributed to the geometric constraints imposed on the μ_3-OH groups bridging to three metal atoms. In addition the steric interactions between the hydrogen-bonded O1···O4 atoms along the Co1−Co3 triangle edge causes expansion of this side of the Co(II) triangle, which forces the two μ_3-OH groups toward the Co_3 plane, thus constraining the *cis* (μ-O)−Co−(μ-O) angle to an average value of 69.1°, more than 20° from the "ideal" value. It similarly compresses the *trans* (μ-O)−Co−N_{pz} bond angles of the Co(μ_3-OH)$_2$(*pz*-N)$_2$ moiety. The *trans* (μ-$O_{phenolate}$)−Co−(μ-$O_{phenolate}$) bond angles are also distorted, with the di-(μ-$O_{phenolate}$)-bridged Co2 having the smallest O−Co−O angle of 162.0(3)°. This almost 20° distortion from the "ideal" is attributable to the bridging of these ligand atoms to Co1 and Co3, bending the (μ-$O_{phenolate}$) atoms toward the other bridged metal center (Co1, Co3) and compressing the O−Co−O angle. The corresponding *trans* O−Co−O bond angles for Co1 and Co3 are considerably less compressed with values of 175.7(4)° and 173.5(3)°, respectively, due to the fact that only one of the *trans* oxygen atom ligands for these two metal atoms originates from a bridging μ-$O_{phenolate}$ group.

Electronic and Magnetic Properties. The electronic spectra and room temperature magnetic moments of **1**−**4** are summarized in Table 7. The room temperature magnetic moments of **1**−**4**, all with magnitudes greater than 4.6, are consistent with values expected for high-spin Co(II) centers.[14] The two lower energy bands in the spectra of **1** and **2** (Table 7) have intensities consistent with spin-allowed d−d transitions, the more intense, higher energy bands in these spectra are indicative of charge-transfer (CT) transition(s). The broad band (500−690 nm) with considerable fine structure in the electronic spectrum of **3** is characteristic of the spin-allowed $^4A_2 \rightarrow {}^4T_1(P)$ d−d transition in a tetrahedral Co(II) crystal field.[14] Only one broad unsymmetrical band is observed in the electronic spectrum with an energy and intensity consistent with CT transition(s). This unsymmetrical band tails considerably to higher wavelengths, thus presumably obscuring the other weak spin-allowed d−d transitions.

Electrochemistry. 1. In CH_2Cl_2, over the scan range +1.8 to −1.8 V at 200 mV s^{-1}, two oxidation waves are observed at $E_p{}^c = +0.24$ and +1.16 V, respectively. Two indistinct reduction "adsorption" features are observed at +0.88 and +0.58 V, indicating complete complex decomposition after the second, higher potential, oxidation. The $E_p{}^c = +1.16$ V feature has been assigned to a ligand (L1) oxidation by comparison to cyclic voltammetry (CV) experiments on uncoordinated L1 in CH_2Cl_2, which exhibits an irreversible oxidation wave at $E_p{}^c = +1.42$ V. Upon metal coordination this wave is shifted to the observed lower potential. Examination of the $E_p{}^c = +0.24$ V wave over the narrower scan range −0.90 V to +0.70 V revealed the presence of a coupled reduction wave at $E_p{}^a = -0.43$ V. The $i_p{}^c/i_p{}^a$ ratio of 2.32 (at 200 mV s^{-1}) and the very large peak to peak separation, $\Delta E_p = 0.67$ V (at 200 mVs^{-1}), indicates that this couple is not quasi-reversible but is attributable to an electrochemical (EC) process. The $E_p{}^c = +0.24$ V wave likely results from a Co(II) → Co(III) oxidation. The oxidized material then undergoes a followup chemical reaction which produces a product that is reduced at $E_p{}^a = -0.43$ V. Attempts to outrun the chemical reaction kinetics of the process at scan rates up to 12 V s^{-1} (using an oscilloscope to record the voltammograms) were unsuccessful, indicating relatively fast EC reaction kinetics.

In CH_2Cl_2, over the scan range +1.8−0 V at 200 mV s^{-1}, oxidation waves are observed for **2** at $E_P{}^c = +0.27$ and +1.22 V along with a small "adsorption" wave at +1.48 V. Numerous reduction "adsorption" features are observed at $E_p{}^a = +1.29$, +0.94 (sh), +0.83, and +0.39 V. The numerous oxidation and reduction "adsorption" waves in the CV indicate that, upon the $E_p{}^c = +1.22$ V oxidation, complete decomposition of the complex occurs. As for **1**, the higher potential, $E_p{}^c = +1.22$ V oxidation wave has been assigned to a ligand (L2) oxidation by comparison to the uncoordinated L2 in CH_2Cl_2, which exhibits an irreversible oxidation wave at $E_p{}^c = +1.28$ V. Investigation of the $E_p{}^c = +0.27$ V wave in the narrower scan range −0.90 to +0.70 V revealed the presence of a coupled reduction wave at $E_p{}^a = -0.11$ V. The nonunity $i_p{}^c/i_p{}^a$ ratio of 4.3 (at 200 mV s^{-1}) and the very large peak to peak separation $\Delta E_p = 0.38$ V (at 200 mV s^{-1}) are indicative of an EC process. The $E_p{}^c = +0.24$ V wave again is assigned to a Co(II) → Co(III) oxidation, the oxidized material of which undergoes a chemical reaction which produces a product that is then reduced at $E_p{}^a = -0.11$ V. Attempts to outrun the reaction (C) kinetics of the EC process at scan rates up to 12 V s^{-1} revealed the development of a new reduction wave (at rates ≥10 V s^{-1})

(14) Nicholls, D. *Comprehensive Inorganic Chemistry, Vol. 3*; Bailar, J. C., Emeleus, H. J., Nyholm, R., Trotman-Dickenson, A. F., Eds.; Pergamon Press: 1973; pp 1087−1093.

Table 7. Summary of Electronic Spectra and Room Temperature Magnetic Moments for Complexes **1**−**4**

complex	electronic band positions, nm (cm^{-1})	extinction coeff, ϵ	proposed band assignment	room temp magnetic moment, μ, μ_b/Co(II)
1·2.5MeOH· 1.5H_2O (in CH_2Cl_2 soln)	636 (15 720)	4.7	d−d	4.64
	464 (21 550)	37.8	d−d	
	368 (27 170)	1650	CT[a]	
2·0.5H_{2O} (in CH_2Cl_2 soln)	528 (18 940)	12.5	d−d	4.68
	434 (23 040)	28.6	d−d	
	358 b sh (27 930)	408	CT	
3 (in MeCN soln)	664 (15 060)	500	$^4A_2 \rightarrow {}^4T_1(P)$	4.47
	612 (16 340)	400	$^4A_2 \rightarrow {}^4T_1(P)$	
	590 w sh (16 950)	280	$^4A_2 \rightarrow {}^4T_1(P)$	
	558 (17 920)	410	$^4A_2 \rightarrow {}^4T_1(P)$	
	530 w sh (18 870)	110	$^4A_2 \rightarrow {}^4T_1(P)$	
4 (in MeCN soln)	454 (20 230)	405	CT	4.85

[a] CT, charge transfer.

between the $E_p^c = +0.24$ V and $E_p^a = -0.11$ V features, presumably the reverse reduction corresponding to the $E_p^c = +0.27$ V oxidation. Thus, the reaction kinetics of the EC process of **2** are slower than those of **1**. The increasing kinetic stability of more highly substituted pyrazolyl ligands has been noted before.[15]

Discussion

The synthesis and characterization of the L1, L2, and L3 ligands described above, indicates that these ligands can be easily made, in acceptable yields, although the conditions necessary to accomplish the second step of the synthesis (Scheme 1) become more vigorous with increasing steric hindrance on the pyrazole rings. This is consistent with the findings of Peterson *et al*.,[9] who reported that reaction of various aldehydes and ketones with bis(3,5-dimethylpyrazolyl) ketone required strongly forcing conditions, *i.e*., temperatures of 160−180 °C, in addition to the presence of $CoCl_2$ catalyst. Indeed, these workers did not report any derivatives of bis(pyrazolyl) ketones with greater than 3,5-dimethyl substitution. Nevertheless, we have managed to react bis(3-isopropylpyrazolyl) ketone with salicylaldehyde, although this reaction requires a temperature of 120 °C, prolonged reaction times (45−60 min), and the presence of excess salicylaldehyde (3 equiv). If these conditions were not used, in particular the excess salicylaldehyde, an uncharacterized polymeric material was obtained.

These new, tridentate, N_2O-donor ligands have significant differences with respect to the tris(pyrazolyl)borates and methanes beyond the ligand donor set. Tris(pyrazolyl)borates form three six-membered chelate rings in a tridentate coordination mode with transition metals, whereas with the (2-hydroxyphenyl)bis(pyrazolyl)methanes, the two pyrazole rings form six-membered rings, but the phenolate arm forms a seven-membered ring. This has consequences with regards to the coordinative properties of these ligands. It appears that with various divalent metals, including Co(II), the reduced coordination properties of the seven-membered phenolate-chelate ring (versus a six-membered ring) are negligible with respect to the formation of 2/1 L/M "sandwich" complexes such as those observed with the unsubstituted L1 and 3,5-dimethyl L2 ligands. However, for the 3-isopropyl-substituted ligand whose pyrazole 3-substitution precludes any possibility of "sandwich" complex formation, no product could be obtained with the phenolate coordinated using $CoCl_2$·6H_2O as a starting material, despite attempts with a variety of reaction conditions. This indicates that the seven-membered-ring chelate which would be formed if phenolate was bound is insufficiently stable to effect displacement of a chloride from the cobalt. With $Co(BF_4)_2$·6H_2O on the other hand, the lack of any strongly coordinating ligand on the metal combined with the propensity of phenolate ligands to act as bridges results in the formation of a tri-phenolate bridged Co(II) trinuclear species (**4**). Complex **4** has an interesting similarity to the di-μ-Cl-bridged Ni(II) trinuclear complex $[Ni_3(\mu_3\text{-Cl})_2(\mu\text{-L3})_2(\text{L3})(\text{MeOH})]Cl$[16] in that it does not have a "closed" $Co_3(\mu\text{-}O_{phenolate})_3$ ring whereas, in contrast, the similarly di-μ_3-OH-bridged Ni(II) system $[Ni_3(\mu_3\text{-OH})_2(\mu\text{-L3})_3][BF_4]$[16] has a "closed" metal−μ-phenolate ring. Examination of Table 6 indicates that the Co(II)−(μ_3-OH) bonds in **4** (average distance: 2.162 Å) are intermediate between the Ni(II)−(μ_3-Cl) bonds of $[Ni_2(\mu_3\text{-Cl})_2(\mu\text{-L3})_2(\text{L3})(\text{MeOH})]Cl$ (average length: 2.512 Å[16]) and the Ni(II)−(μ_3-OH) bonds of $[Ni_3(\mu_3\text{-OH})_2(\mu\text{-L3})_3][BF_4]$ (average: 2.057 Å[16]). The Co(II)−(μ_3-OH) bonds in **4** may be sufficiently long to expand the sides of the Co_3 triangle enough to preclude complete $Co_3(\mu\text{-}O_{phenolate})_3$ ring formation resulting in the observed structure with two phenolate bridges and one "broken-bridge" terminal phenolate (Figure 5); a structure more analogous to that of $[Ni_2(\mu_3\text{-Cl})_2(\mu\text{-L3})_2(\text{L3})(\text{MeOH})]Cl$ than that of $[Ni_3(\mu_3\text{-OH})_2(\mu\text{-L3})_3][BF_4]$ despite its similar potential bridging ligand (μ-O_5) donor set.

Acknowledgment. This work was supported by Grant AI-1157 from the Robert A. Welch Foundation. The NSF-ILI program grant USE-9151286 is acknowledged for partial support of the X-ray diffraction facilities at Southwest Texas State University. Dr. R. Bhalla is also thanked for his assistance in performing searches of the Cambridge Crystallographic Database.

Supporting Information Available: Complete list of atomic positions, bond lengths and angles, anisotropic thermal displacement parameters, hydrogen atom coordinates, data collection and crystal parameters, and ORTEP plots showing complete atomic labeling for **L1**, **1**, **2**, **3**, and **4** (49 pages). Ordering information is given on any current masthead page.

IC9610703

(15) Mohan, M.; Holmes, S. M.; Butcher, R. J.; Jasinski, J. P.; Carrano, C. J. *Inorg. Chem.* **1992**, *31*, 2029.

(16) Higgs, T. C.; Carrano. C. J. *Inorg. Chem*. **1997**, *36*, 298.